DOI: 10.1002/chem.200701862

Molecular Pacman: Folding, Inclusion, and X-ray Structures of Tri- and Tetraamino Piperazine Cyclophanes

Kari Raatikainen, Juhani Huuskonen, Erkki Kolehmainen, and Kari Rissanen*[a]

Abstract: Reaction of piperazine and 1,3-bis(bromomethyl)-2-nitrobenzene under high-dilution conditions yields cyclic trimeric trinitro, tetrameric tetranitro, and pentameric pentanitro piperazine cyclophanes. Reduction of the nitro groups with $SnCl_2$ under acidic conditions produces the corresponding triamino and tetraamino piperazine cyclophanes. The solution studies of both nitro and amino piperazine cyclophanes at 30 °C by ^1H NMR spectroscopy shows symmetrical structures owing to the fast conformational exchange, whereas the low temperature studies of the tetraamino piperazine cyclophane reveals interesting dynamic behavior that indicates additional intramolecular interactions. Careful crystallizations of the trimeric trinitro and triamino and the tetrameric tetraamino cyclophanes resulted in crystals suitable for X-ray diffraction studies. In the crystalline state the amino-functionalized cyclophanes manifest an extraordinary circular intramolecular hydrogen-bonding network that leads to a fixed 3D structure. Hydrogen bonding in the triamino trimer leads to orientation of all three of the amino groups on the same side of the macrocycle, namely, the *rcc* conformation, whereas the tetraamino tetramer folds into a more compact shell-like conformation. During the crystallization process one acetonitrile guest is enclosed into the cavity of the tetraamino cyclophane, which gives a crystalline inclusion complex with remarkable resemblance to the famous Pacman motif. The folding, which mimics the behavior of some cyclic peptides and pyrroles, is induced by intramolecular hydrogen bonding from the amino groups to the tertiary amine groups of the piperazines. The cavity of the tetraamino tetramer is markedly smaller than in the corresponding, but nonfolded, tetranitro tetramer and the guest/host volume ratio (packing coefficient) for the acetonitrile and the cavity is approximately 50%, which indicates a good size match for acetonitrile inclusion.

Keywords: cyclophanes · hydrogen bonds · inclusion compounds · nitrogen heterocycles · X-ray diffraction

Introduction

Intensive research over recent years in the area of host-guest chemistry has set high demands on designing more advanced structural features and functionalities for macrocyclic host compounds. Our attention has been focused on the design of structurally reinforced macrocycles, such as resorcinarenes.[1] Recently we have turned our interest back to piperazine subunits[2] instead of the more commonly used ethylenediamine moiety in azacrown-type cyclophanes. Piperazine, which is a cyclic bis-secondary amine compound with a 1,4-diazacyclohexane skeleton, easily undergoes N-alkylation reactions with bis-functionalized electrophiles, which leads to highly preorganized, often quite rigid, cyclophanes with binding sites and cavities for a variety of guests.[3]

The importance of preorganization and rigidity is manifested in many macrocycles, for example, resorcinarenes can bind suitably sized quests through cation–π or C–H···π interactions[4] or spherands selectively bind Li^+ and Na^+ ions owing to an excellent size match and favorable spatial orientation of the donor atoms.[5] Piperazine moieties have been effectively used for rigidification and preorganization, as demonstrated by Kihara and co-workers in their highly selective Li^+ host.[6] Piperazine has generally been incorporated into small tetradentate azamacrocycles to improve size selectivity for transition metals. In these complexes the piperazine has been found to exist in the boat conformation.[3b,7] In larger piperazine-based macrocyclic structures the piperazine adopts the energetically more favorable chair conformation,[8] in which the N-substituents are in the equa-

[a] M.Sc. K. Raatikainen, Dr. J. Huuskonen, Prof. Dr. E. Kolehmainen, Prof. Dr. K. Rissanen
Nanoscience Center, Department of Chemistry
University of Jyväskylä, Survontie 9
P.O. Box 35, 40014 JYU (Finland)
Fax: (+358) 14-260-2651
E-mail: Kari.Rissanen@jyu.fi

torial positions. These cyclophanes are generally prepared by nucleophilic substitution with suitable benzylic halides under high dilution conditions.[2,9,10] Also larger spacers, such as azobenzene units, have been used instead of benzene to introduce larger ring size and photoresponsive functionality.[2d] Piperazine-based macrocycles are known to form inclusion complexes with small guests, typically solvent molecules.[2a,d,e,10] Macrocyclic transition-metal complexes have also been reported.[2b,11] Herein we report the synthesis and characterization of three new piperazino cyclophanes with different sizes and functional groups. The solution structures and dynamic behavior was studied by ^{1}H NMR spectroscopy and the solid-state structures of the macrocycles and their inclusion complexes were investigated with single-crystal X-ray diffraction.

Results and Discussion

The synthesis route to cyclophanes **3** to **7** is depicted in the Scheme 1. Trinitro trimer **3** was synthesized by using a modification of our published procedures from piperazine **1** and 1,3-bis(bromomethyl)-2-nitrobenzene **2**.[2a,e] The synthesis was performed under high-dilution conditions in a mixture of THF/acetonitrile in the presence of excess potassium carbonate (see Experimental Section). A mixture of cyclo-

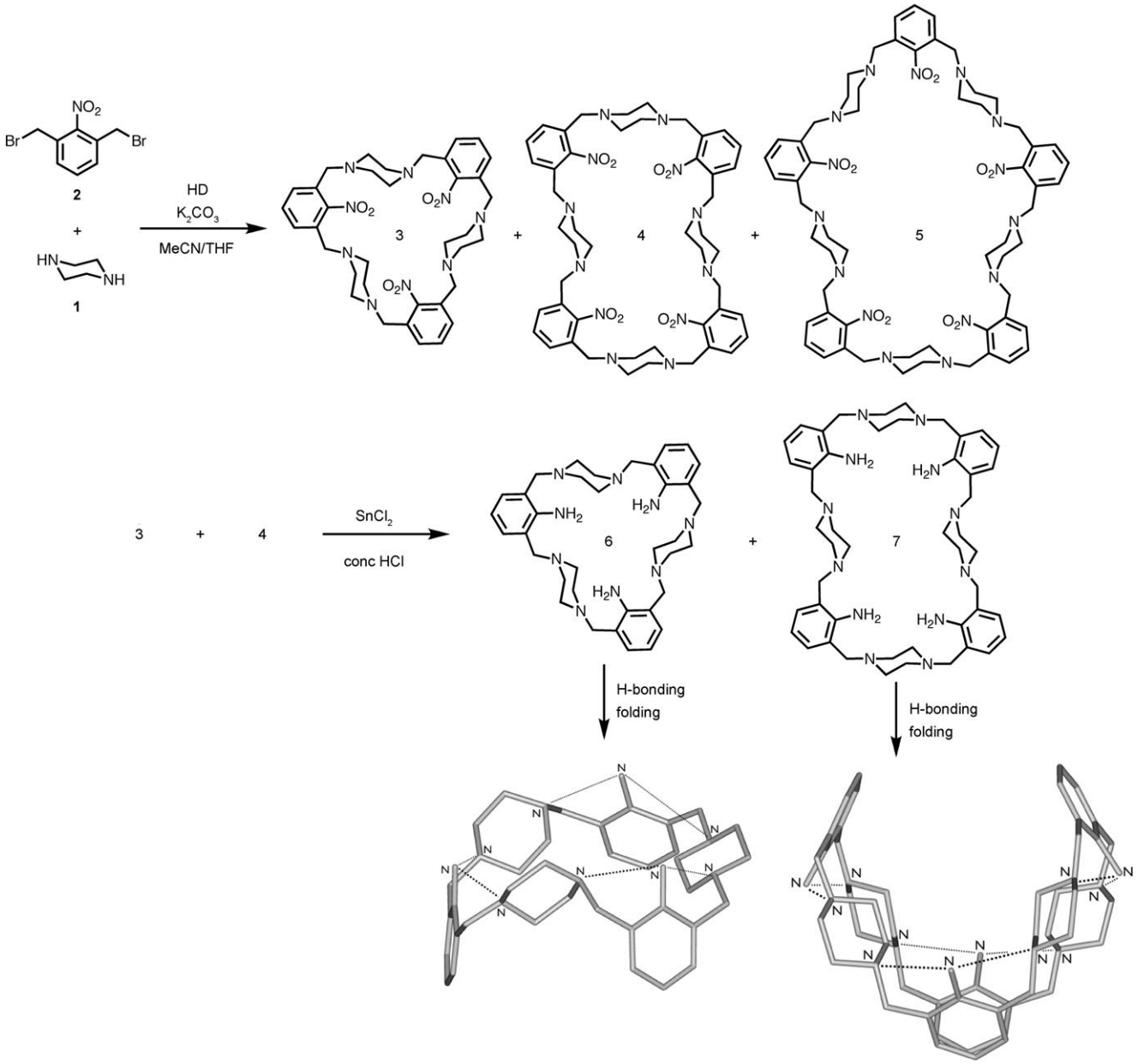

Scheme 1. Synthetic route for the preparation of cyclophanes **3** to **7**. Hydrogen bonding and folding in **6** and **7** are also shown.

phanes **3**, **4**, and **5** was isolated in an overall yield of 35%, but owing to difficulties in the purification step, the isolated yields for **3** and **4** were only 8 and 3%, respectively. Pentanitro pentamer **5** was only separated as a minor product during silica gel column chromatography and identified by means of TLC and ESI-MS analyses. Triamino trimer **6** and tetraamino tetramer **7** were synthesized by reduction of the nitro groups with tin(II) chloride in concentrated hydrochloric acid and isolated in yields of 66 and 72%, respectively.

The ^{1}H NMR spectroscopy study of **3** at 30°C suggests a highly symmetrical structure in which the signals from three aromatic protons are averaged into one singlet. Also piperazine protons are shown as one broad singlet. Crystallization from a mixture of acetonitrile/CH_2Cl_2 (1:1) produced crystals that were suitable for X-ray diffraction. The X-ray structure of **3** is shown in Figure 1. As expected, the piperazine units are in the energetically preferred chair conformation and the nitro groups of the aryl spacers have a *syn–anti–anti* conformation. The cavity in **3** is too small and deformed to include even the small acetonitrile solvent molecule and is also blocked by the short intramolecular O44···O50 distance (4.95 Å).[13] Within the crystal lattice, the cavity in **3** is blocked by the aryl rings and nitro groups of the adjacent molecules, which leaves insufficient space for inclusion of any solvent molecule.

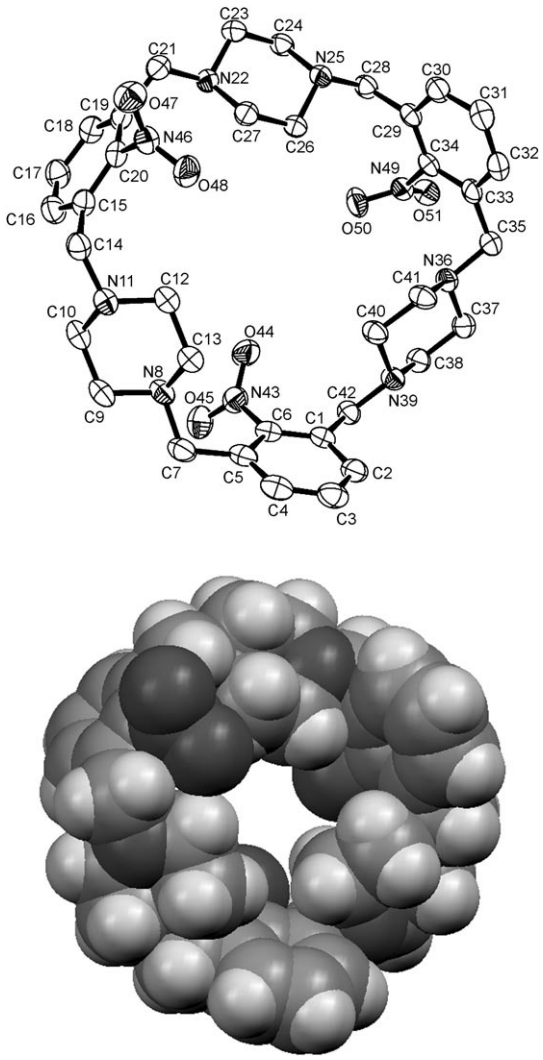

Figure 1. An ORTEP plot showing the numbering scheme (top) and a van der Waals (VDW) representation (bottom) of **3**. Hydrogen atoms are omitted for clarity and ellipsoids are drawn at the 40% probability level.

Reduction of the nitro groups in **3** to give triamino trimer **6** changes the appearance of the aryl protons in the ^{1}H NMR spectrum, which now has a triplet at $\delta = 6.55$ ppm and a doublet at $\delta = 6.94$ ppm, compared with the singlet for **3**. Recrystallization from a mixture of acetonitrile/CH_2Cl_2 (1:1) produced crystals that were suitable for X-ray diffraction (Figure 1. Like trimer **3**, compound **6** also did not form an inclusion complex with a solvent molecule owing to the twisting and small size of the cavity. Compound **6** has an exceptional all *syn* conformation of the three amino groups as a result of intramolecular hydrogen bonds between the lone pairs of the piperazine nitrogen atoms and the hydrogen atoms of the amino group. Intramolecular hydrogen bonding strongly affects the conformations of the piperazine units. In contrast with **3**, two of the piperazine units in **6** have adopted a less-favored conformation in which the N39···C42 and N22···C21 bonds are axial instead of in the sterically more favorable equatorial orientation (Figure 2).

Because of steric demands for the perfect circular hydrogen bonding array cannot be met owing to the small size of **6**, the remaining piperazine unit relaxes the strain by adopting the more favorable conformation with equatorial nitrogen substituents, which explains the absence of a sixth hydrogen bond between N43 and N8. A completely circular hydrogen-bonding array would require that one nitrogen substituent in all three piperazine units would have to be in an axial position, which is sterically impossible in **6**. The hydrogen bond distances range from 2.836(3) to 2.940(3) Å (Table 1), which suggests a moderately strong interactions.[14] The protonation of **6** forms a hexaammonium cation and preliminary molecular modeling studies reveal a perfectly preorganized binding site for tetrahedral triply charged anions, such as PO_4^{3-}, through strong hydrogen bonding to the protonated N43, N44, and N45 atoms. Detailed complexation and modeling studies with various anionic guests will be reported elsewhere.

Recrystallization of **6** from CH_2Cl_2/methanol mixture resulted in us obtaining the crystal structure of the methanol solvate **6**·MeOH. As in **6**, the amino groups in **6**·MeOH occupy the same side of the cyclophane and a methanol molecule is bound to one of the amino groups with a weak hydrogen bond (N44-H44B···O46, 3.045(4) Å; Figure 3). The cyclophane skeleton retains its configuration despite the methanol binding and leading to the breakdown of one of the hydrogen bonds. The cavity of **6** is too small to include the methyl group of the methanol, and thus, it is located on the top of the macrocyle.

The synthesis (Scheme 1) results in a mixture of **3**, **4**, and **5**. In our previous study on the same system we reported the crystal structure of **4**·MeCN.[2a] The crystals were grown

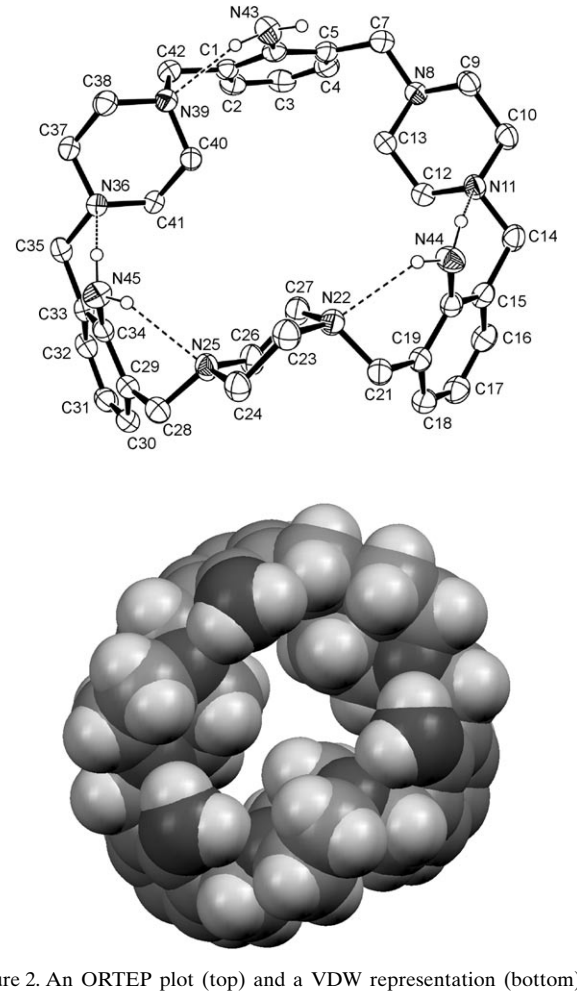

Figure 2. An ORTEP plot (top) and a VDW representation (bottom) of **6**. Hydrogen atoms (except for -NH_2) are omitted for clarity, hydrogen bonds are shown with dotted lines, and the thermal displacement parameters are shown at the 40% probability level.

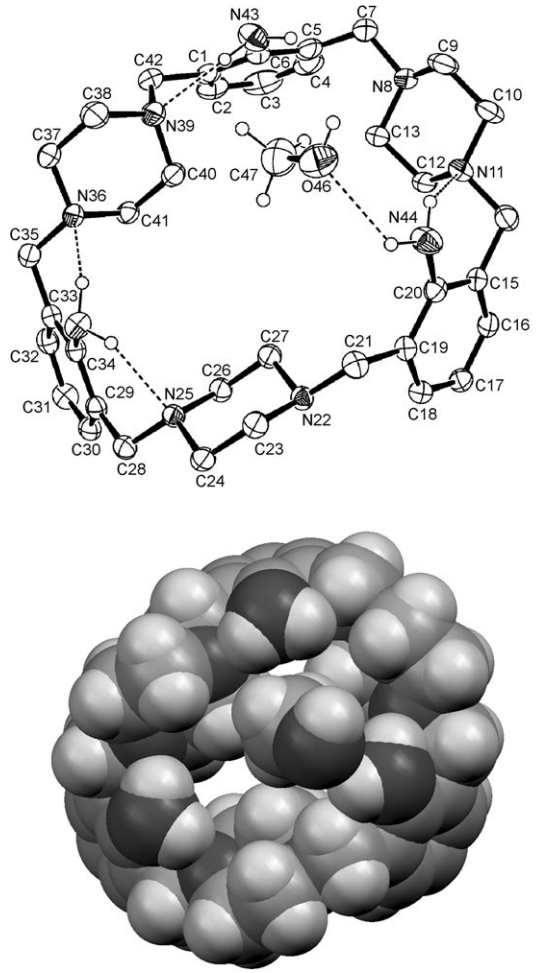

Figure 3. An ORTEP plot (top) and a VDW representation (below) of **6**·MeOH. Hydrogen atoms (except for -NH_2) are omitted for clarity, hydrogen bonds are shown with dotted lines, and the thermal displacement parameters are shown at the 40% probability level.

from a solution in acetonitrile/ethanol. Cyclophane **4** has a rigid 36-membered ring with a large, roughly ellipsoidal cavity. As for **4**, our previous studies on other large piperazine cyclophanes have shown that solvent molecules are easily included into the cavity.[2] Although the volume of the cavity in **4** is difficult to reliably measure, a value of approximately 190 Å^3 was obtained from a calculation by using PLATON (VOIDS).[15] Figure 4 shows the X-ray structure of the inclusion complex with one acetonitrile guest. The cavity is too small to simultaneously include two acetonitrile molecules (the molecular volume of acetonitrile is 53.2 Å^3)[16] and thus the molecule that is included is located in the corner of the cavity. The nitro groups in **4** symmetrically occupy the upper and lower parts of the cyclo-

Table 1. Hydrogen bonds lengths [Å] and angles [°] between specific donors and acceptors in **6**, **6**·MeOH and **7**@MeCN·2CH_2Cl_2.

	6		**6**·MeOH		**7**@MeCN · 2CH_2Cl_2	
D–H···A	*d*	∢	*d*	∢	*d*	∢
N43–H43B···N39	2.849(3)	139(3)	2.824(4)	137(4)		
N44–H44A···N11	2.940(3)	135(2)	2.931(4)	137(4)		
N44–H44B···N22	2.926(3)	136(2)	–	–		
N45–H45A···N25	2.922(3)	135(2)	2.853(3)	140(3)		
N45–H45B···N36	2.836(3)	139(2)	2.867(4)	137(3)		
N44–H44B···O46	–	–	3.045(4)	129(3)		
O46–H46···N8[a]	–	–	2.878(4)	164(3)		
N57–H57A···N53					2.970(5)	139(5)
N57–H57B···N8					2.956(5)	138(4)
N58–H58B···N22					2.828(6)	136(4)
N58–H58A···N11					2.934(6)	139(4)
N59–H59B···N25					2.989(5)	133(5)
N59–H59A···N36					2.899(6)	140(4)
N60–H60B···N39					2.897(6)	136(4)
N60–H60A···N50					2.873(6)	135(4)

[a] Symmetry transformations used to generate equivalent atoms: $-x+3/2,y+1/2,-z+3/2$.

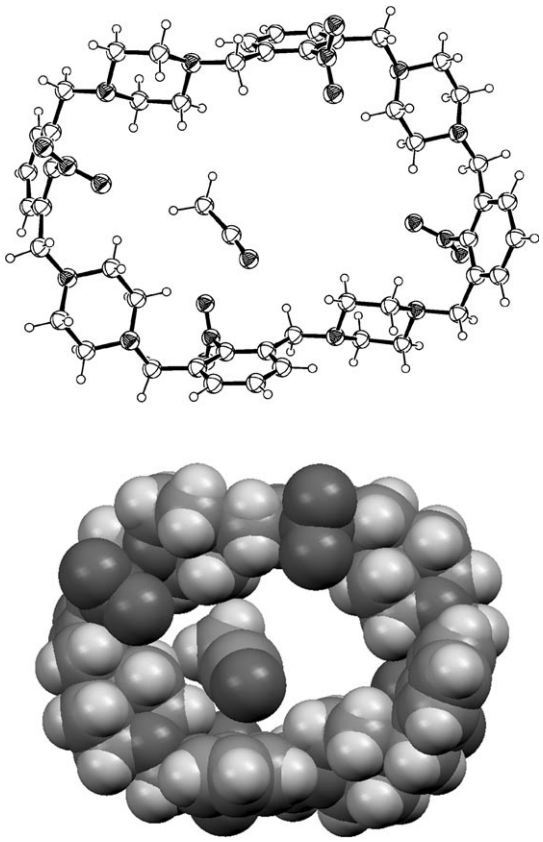

Figure 4. An ORTEP plot (top) and a VDW representation (below) of **4**·MeCN.[2a]

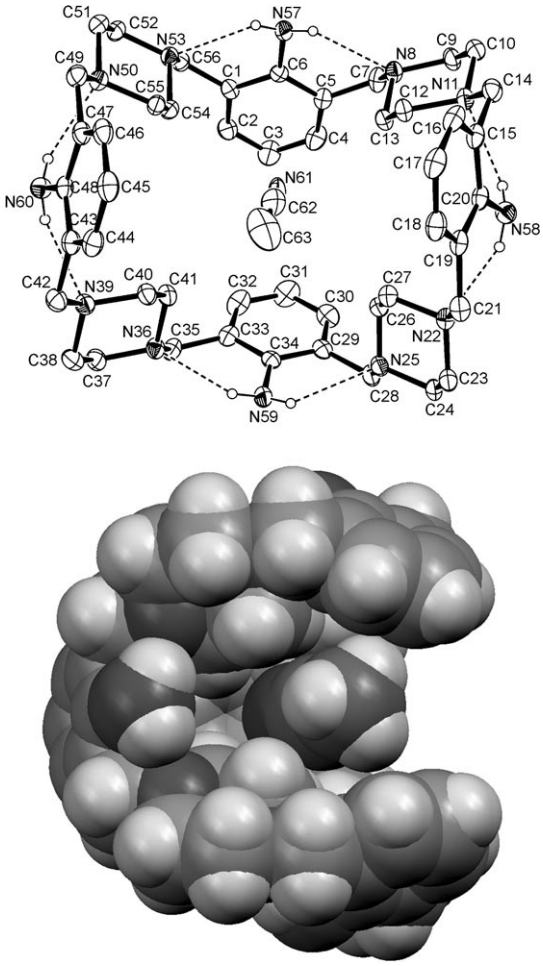

Figure 5. An ORTEP plot (top) and a VDW representation (below) of **7**@CH_3CN·2 CH_2Cl_2. Two CH_2Cl_2 molecules and hydrogen atoms (except amino hydrogen atoms) are omitted for clarity, and the thermal displacement parameters are shown at 30% probability level.

phane, which leads to the *anti–anti–syn–syn* conformation of the nitrobenzene spacers.[2a]

The four nitro groups in **4** were reduced (Scheme 1) to the corresponding amino groups and cyclophane **7** was obtained. Recrystallization from a mixture acetonitrile/CH_2Cl_2 (1:1) led to the formation of crystals that were suitable for X-ray diffraction. The X-ray structure revealed a drastic change in the overall conformation of the cyclophane with simultaneous encapsulation of an acetonitrile molecule. In addition two CH_2Cl_2 molecules were found to reside in the crystal lattice. Figure 5 shows a plot of **7**@MeCN·2 CH_2Cl_2 in which the cyclophane has folded into a shell-like conformation. The resemblance to the famous NAMCO video game motif Pacman[17] from 1980s is striking. Folding of the cyclophane follows the same pattern as that for trimer **6**, but as a result of the larger size and more flexible nature of the tetramer, the 3D structure of **7** is completely different from that of corresponding tetranitro analogue **4** (Figure 4.). The *anti–syn–anti–syn* conformation and the larger number of aminophenyl spacers in **7** provides enough space for the optimal conformation for all piperazine subunits, that is, all nitrogen substituents are in equatorial positions and all of the free electron pairs of the nitrogen atoms are involved in hydrogen bonding. The hydrogen-bonding pattern is shown in Figure 5 and the distances and angles are listed in Table 1.

The hydrogen bonds in **7** form a cyclic array, which is typical for self-folding cavitands and provides additional stabilization through co-operative effects.[18] The folding in **7** is unique for piperazine-based cyclophanes, whilst a figure-of-eight motif is sometimes observed in cyclic peptides[19] and pyrroles[20] and is the simplest example of intramolecular folding of a large macrocycle. Among the non-natural cyclopeptides, the tryptophane derived 22-membered macrocycle has been shown to fold into a left-handed double helix.[21] The figure-of-eight motif is a helical arrangement, in which the major controlling factor appears to be stabilization as a result of intramolecular hydrogen bonding or aromatic π–π interactions. The geometric constraints in the cyclic structures greatly reduce the conformational freedom and for those molecules of a suitable size, flexibility and intramolecular interactions leads to the formation of a figure-of-eight motif.[19–21]

The volume of the roughly spherical cavity in **7** (after removal of the enclosed acetonitrile) is 110 $Å^3$ (calculated with PLATON).[15] This volume is approximately 45%

smaller than the corresponding cavity of **4** despite the fact that both tetramers have identical spacer connections and formal ring sizes. The cavity is approximately 9.7 Å deep and the bottom of it is almost closed because the C3···C31 distance is 3.83 Å (see Figure 5). The methyl part of the acetonitrile guest is loosely pinched between two aryl groups with a distance of 3.860(7) Å (C44···C63) and a weak C–H···π interaction of 3.953(8) Å (C63···C18). The C≡N moiety of the acetonitrile guest has weak interactions to the methylene groups of the piperazine spacers with distances of 3.642(6) (C54···N61) and 3.546(6) Å (N61···C13).

The ^{1}H NMR spectrum of **7**@CH_3CN in $CDCl_3$ shows that the resonance of acetonitrile is deshielded by only 0.1 ppm compared with the shift of acetonitrile itself in $CDCl_3$ at $\delta =$ 2.10 ppm,[22] thus indicating very weak or vanishing intermolecular interactions between **7** and the acetonitrile guest in chloroform. Therefore, the formation of **7**@CH_3CN revealed by the X-ray structure must happen during folding and crystallization of the cyclophane. Additional proof for inclusion of the acetonitrile guest during folding was obtained by dissolving the crystals of **7**@MeCN·2CH_2Cl_2, in pure $CDCl_3$ in an NMR tube. After dissolution and subsequent slow evaporation of the solvent, new crystals formed. These crystals have a new different, triclinic crystal lattice (space group $\bar{P}1$) containing now chloroform instead of dichloromethane as the lattice solvent, but still forms the same folded structure with acetonitrile included into the cavity. The size match analysis of the guest in the cavity was carried out by calculating the packing coefficient of the cavity (PC_{cavity}) in **7**. PC_{cavity} is defined as V_{vdw}/V_{cavity} and was introduced by Mecozzi and Rebek, in which V_{vdw} is the van der Waals volume and V_{cavity} is the volume of the cavity.[23] They reported that inclusion into the cavity is largely determined by host–guest volume-fit and they found that in the liquid phase the most favorable PC_{cavity} is $(55\pm9)\%$. In the solid state the corresponding PC_{cavity} is $(63\pm9)\%$.[23] For Pacman complex **7**, the PC_{cavity} is very close to 50%, which is in a good agreement with literature values that range from 29 to 64% for similar inclusion complexes.[24]

Dynamic characteristics of **7** were also examined in solution through variable-temperature NMR spectroscopy experiments. The ^{1}H NMR spectra in $CDCl_3$ were recorded in the temperature range from +30 °C to −60 °C, and the effect of temperature on the spectra is illustrated in Figure 6. At +30 °C, the resonances from the benzylic and piperazine ring protons were time-averaged into the singlets at $\delta = 3.56$ and 2.18 ppm, respectively, owing to the conformational equilibrium in the fast-exchange regime. Below −10 °C, the signal of the benzylic protons ($\delta = 3.56$ ppm at 30 °C) started to divide into two resonances at $\delta = 4.02$ (**a**) and 3.11 ppm (**b**) and the piperazine signal ($\delta = 2.18$ ppm at 30 °C) gave rise to four resonances at $\delta = 2.91$ (**c**), 2.24 (**d**), 2.05 (**e**), and 1.53 ppm (**f**). From this resonance pattern, most clearly resolved in the spectrum at −60 °C, one can conclude that the slow chair–chair interconversion of the piperazine unit makes its axial and equatorial protons nonequivalent. These are further divided into two resonances

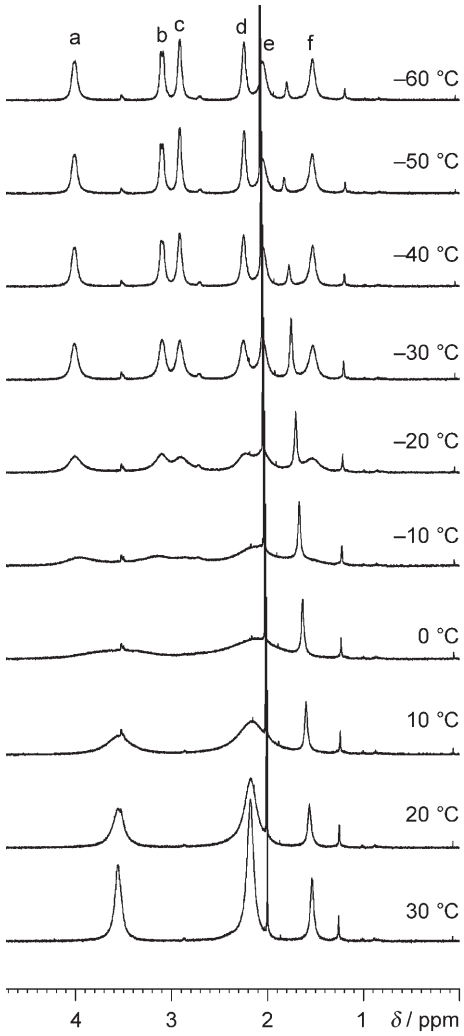

Figure 6. Selected part of the temperature-dependent ^{1}H NMR spectra of **7**@MeCN·2CH_2Cl_2 in chloroform.

by sterically hindered rotation around the C–C axis of the benzylic system, which furthermore makes its methylene protons diastereotopic and inequivalent.

Also the integrals of signals **e** and **f** become smaller compared with those of **c** and **d** (Figure 6.) along with decreasing thermal motion, which indicates that the conformers participating in the dynamic processes are energetically unequal. This inequivalence is suggested to arise from the hydrogen-bond-stabilized conformation, which is close to the conformation in crystalline state shown in Figure 5. When the piperazine subunit is rotated 180° around the C–C axis, hydrogen bonding is hindered. Also the NH_2 signal at $\delta =$ 5.76 ppm shows increased broadening at temperatures below −30 °C, which refers to the increased hydrogen-bond interactions.

Conclusion

The use of piperazine and functional or prefunctional spacer groups offers a straightforward route for preparing functional piperazine cyclophanes of various sizes. The nitro group in an aromatic spacer does not lead to N-alkylation during the synthesis and thus results in nitro-functionalized piperazine cyclophanes. The synthetically feasible reduction of the nitro group to a more versatile amino group opens up further possibilities for the functionalization of the cyclophanes. The spatial proximity of the hydrogen-bond donating amino group and the tertiary amine as the hydrogen-bond acceptor in piperazine moieties leads to unprecedented intramolecular interactions that have a dominating effect on the overall conformation of the cyclophane. In the sterically more strained trimeric cyclophane, the size of the macrocycle is too small to allow the formation of a completely circular hydrogen-bonding pattern, whereas in the larger tetramer this is possible. In the trimer intramolecular hydrogen bonding forces the amino groups into the all-*syn* conformation, thus allowing the construction of a functional site, for example, for metal-ion coordination at the same side of the cyclophane The same hydrogen-bonding interactions, but now forming a complete circle, in the larger and slightly more flexible tetramer leads to the folding of the cyclophane into a shell-like tertiary structure capable of enclosing an acetonitrile molecule inside the cavity formed in the crystalline state. As a result of intramolecular hydrogen bonding observed in these compounds, new tertiary structures or spatial orientation of functional groups for large macrocycles can be designed and used to construct spatially directed functionalities or new properties as a result of the folding process.

Experimental Section

General methods: All chemicals and solvents were reagent grade, purchased commercially, and used as received. 1,3-Bis(bromomethyl)-2-nitrobenzene **1** was synthesized by radical bromination of 1,3-dimethyl-2-nitrobenzene with *N*-bromosuccinimide.[26] Melting points were measured with Mettler Toledo FP62 apparatus. ^{1}H and ^{13}C NMR spectra were recorded by using Bruker Avance DPX 250 and DRX 500 FT NMR spectrometers operating at 250 and 500 MHz, respectively, for the ^{1}H NMR spectra and at 63 and 126 MHz, respectively, for the ^{13}C NMR spectra. All samples were prepared in $CDCl_3$ at 30 °C unless otherwise stated (using the residual solvent peak at $\delta = 7.26$ ppm and the center peak at $\delta = 77.00$ ppm from TMS as internal references for the ^{1}H and ^{13}C NMR spectra, respectively). Mass spectra were obtained by using a Micromass (ESI-TOF) spectrometer. The high dilution syntheses were performed with an Isco WIZ peristaltic pump. Column chromatography was performed with Merck silica gel 60 (0.040–0.063 mesh) and TLC was performed on Alugram sil G/UV$_{254}$ plates. Elemental analyses were carried out by using a VariolEL instrument from Elementar Analysensysteme.

X-ray analysis:[27] Colorless crystals of trimers **3**, **6**, and tetramer **7** for single-crystal X-ray diffraction analyses were grown in a mixture of CH_2Cl_2 and acetonitrile by slow solvent evaporation. Trimer **6** was also recrystallized from methanol/CH_2Cl_2 to give a methanol-solvate crystal structure. Suitable crystals were selected and analyses were performed by using a Bruker Kappa Apex II diffractometer with graphite-monochromatized $Mo_{K\alpha}$ ($\lambda = 0.71073$ Å) radiation for macrocycles **6** and **7**, and graphite-monochromatized $Cu_{K\alpha}$ ($\lambda = 1.54184$ Å) radiation for macrocycle **3**. Collect software[28] was used for the data measurement and DENZO-SMN[29] software was used for data processing. The structures were solved by direct methods with SIR97[30] and refined by full-matrix least-squares methods with WinGX-software,[31] which utilizes the SHELXL-97 module.[32] All C–H hydrogen positions were calculated by using a riding atom model and N–H hydrogen atoms were located from the electron density map after anisotropic refinement of non-hydrogen atoms. Crystallographic data for **3**, **6**, **6**·MeOH and **7**@MeCN·2 CH_2Cl_2 is reported in Table 2.

Synthesis

*1,5,9(2)-Trinitro-1,5,9(1,3)-tribenzena-3,7,11(1,4)-tripiperazinacyclophane (**3**)*: Compound **3** was synthesized by using a modification of procedures published for similar compounds.[2a,e] 1,3-Bis(bromomethyl)-2-nitrobenzene **2** (5.13 g, 16.61 mmol) was dissolved in acetonitrile (500 mL). Piperazine **1** (1.43 g, 16.61 mmol) was dissolved in the mixture of THF (400 mL) and acetonitrile (100 mL). These solutions (500 mL, 0.33 mM)

Table 2. Crystallographic data for **3**, **6**, **6**·MeOH, and **7**@MeCN·2 CH_2Cl_2.

Cyclophane	**3**	**6**	**6**·MeOH	**7**@MeCN·2 CH_2Cl_2
formula	$C_{36}H_{45}N_9O_6$	$C_{36}H_{51}N_9$	$C_{37}H_{55}N_9O$	$C_{52}H_{75}Cl_4N_{13}$
M_w [g mol^{-1}]	699.81	609.86	641.90	1024.05
T [K]	173.0(1)	173.0(1)	173.0(1)	173.0(1)
wavelength [Å]	1.54184	0.71073	0.71073	0.71073
crystal system	triclinic	monoclinic	monoclinic	monoclinic
space group	$P\bar{1}$	$P2_1/n$	$P2_1/n$	$P2_1/c$
a [Å]	12.523(3)	12.595(6)	12.2265(8)	19.243(4)
b [Å]	13.196(3)	11.343(5)	11.8992(6)	12.129(4)
c [Å]	13.816(2)	23.55(1)	25.084(3)	23.801(5)
α [°]	98.14(1)	90	90	90
β [°]	110.17(1)	98.038(4)	90.444(4)	92.382(2)
γ [°]	116.928(9)	90	90	90
V [Å^3]	1785.6(6)	3332(3)	3649.2(5)	5550(2)
ρ_{calcd} [g cm^{-3}]	1.302	1.216	1.168	1.225
Z	2	4	4	4
μ [mm^{-1}]	0.744	0.075	0.073	0.260
$F(000)$	744	1320	1392	2184
crystal size [mm^3]	0.3x0.3x0.3	0.3x0.2x0.2	0.3x0.2x0.2	0.3x0.3x0.2
θ range [°]	3.65–63.42	2.43–25.00	2.94–25.00	1.06–25.00
reflns collected	7824	11061	9377	16414
reflns unique	5776	5856	6413	9764
$R_{(int)}$	0.0631	0.0464	0.1050	0.0577
data	5776	5856	6413	9764
restraints	0	16	15	39
parameters	461	431	450	673
GOF on F^2	1.052	1.070	1.125	1.044
final R indices [$I > 2\sigma(I)$]	$R_1 = 0.0514$, $wR_2 = 0.1325$	$R_1 = 0.0519$, $wR_2 = 0.1073$	$R_1 = 0.0755$, $wR_2 = 0.1314$	$R_1 = 0.0907$, $wR_2 = 0.2257$
R indices (all data)	$R_1 = 0.0638$, $wR_2 = 0.1436$	$R_1 = 0.0828$, $wR_2 = 0.1242$	$R_1 = 0.1094$, $wR_2 = 0.1492$	$R_1 = 0.1347$, $wR_2 = 0.2631$
ΔF peak/hole [e Å^{-3}]	0.23/−0.21	0.20/−0.15	0.31/−0.30	0.87/−1.07

were added into the mixture of acetonitrile (400 mL), THF (100 mL), and potassium carbonate (25 g, 180 mmol) heated at reflux by using a peristaltic pump with a flow rate of 30 mL h^{-1}. The mixture was heated at reflux for a total of 24 h and filtered hot. The solution was concentrated to a volume of 1000 mL and allowed to stand in a refrigerator overnight. Solid and colored impurities were filtered with activated charcoal. The clear-yellowish solution was evaporated to dryness and the white residue was dissolved in CH_2Cl_2 (30 mL). After filtering insoluble impurities, hexane (10 mL) was added and the product was recrystallized to give white crystals, while standing at room temperature. (440 mg, 11%). Decomposition under 300°C; ^{1}H NMR: $\delta = 7.33$ (s, 9H), 3.34 (s, 12H), 2.30 ppm (s, 24H); ^{13}C NMR: $\delta = 151.6$, 130.9, 130.1, 129.7, 57.8, 52.7 ppm; MS: *m/z*: 700.4 [$M+H^+$], 722.3 [$M+Na^+$], 738.3 [$M+K^+$]; elemental analysis calcd (%) for $C_{36}H_{45}N_9O_6 \cdot {}^1/_8 CH_2Cl_2$: C 61.08, H 6.42, N 17.74%; found: C 61.29, H 6.46, N 17.46.

*1,5,9,13(2)-Tetranitro-1,5,9,13(1,3)-tetrabenzena-3,7,11(1,4)-tetrapiperazinacyclophane (**4**)*: Compound **4** was synthesized as described above by using a modified work up, which also provide an alternative synthetic route for **3**. The high-dilution reaction was performed by dissolving **2** (7.50 g, 24.28 mmol) and **1** (2.10 g, 24.38 mmol) in THF (500 mL) and acetonitrile (500 mL), respectively. The solutions were added simultaneously with dropping funnels over 10 h into the boiling mixture of acetonitrile (500 mL) and potassium carbonate (32 g, 230 mmol). The resulting mixture was heated at reflux for an additional 2 h and evaporated to dryness. The residual solid was mixed with CH_2Cl_2 (100 mL), filtered, and thoroughly rinsed to dissolve all of the macrocycles. The yellowish filtrate was mixed with silica gel and evaporated to dryness. The remaining solid was poured onto a short silica gel column and rinsed first with a mixture of THF/hexane (1:2) (200 mL), followed by elution of the product mixture (2.0 g, 35%) of **3, 4** and **5** (minor) with a mixture of THF/hexane/CH_2Cl_2 (1:2:3). Macrocycles **3** and **4** were isolated by fraction precipitation. Macrocycle **3** was crystallized from the mixture of chloroform and *n*-hexane as a white powder by standing at room temperature (467.8 mg, 8%). Macrocycle **4** was crystallized as a white crystals from a mixture of chloroform/acetonitrile (1:1) at room temperature (187.3 mg, 3%). Decomposition under 300°C; ^{1}H NMR: $\delta = 7.41$–7.31 (m, 12H), 3.41 (s, 16H), 2.36 ppm (s, 32H); ^{13}C NMR $\delta = 151.3$, 130.5, 193.0, 129.7, 57.6, 53.0 ppm; MS: *m/z*: 933.4 [$M+H^+$], 955.5 [$M+Na^+$].

*1,5,9(2)-Triamino-1,5,9(1,3)-tribenzena-3,7,11(1,4)-tripiperazinacyclophane (**6**):* Compound **6** was prepared by using a modification of a procedure published for similar compounds.[33] Compound **3** (0.60 g, 0.86 mmol) was dissolved in a solution of concentrated HCl (10 mL) and tin(II) chloride (6.00 g, 26.59 mmol) at 0°C. The suspension formed was mixed at room temperature under nitrogen for 20 min, heated in a boiling water bath for 20 min, and allowed to cool under a flow of nitrogen for another 20 min. The cooled suspension was filtered and the solid material was rinsed with acetone (5 mL) and CH_2Cl_2 (5 mL). The crude product was neutralized with a mixture of water (5 mL) and concentrated aqueous ammonia (10 mL) and extracted with CH_2Cl_2. The solution was dried with Na_2SO_4 and concentrated to a volume of 5 mL. Hexane (2 mL) was added and the solution was allowed to evaporate at room temperature to give a white crystalline product (343 mg, 66%). Decomposition under 300°C; ^{1}H NMR: $\delta = 6.94$ (d, ^3J(H,H) = 7.42 Hz, 6H), 6.55 (t, ^3J(H,H) = 7.42 Hz, 3H), 5.40 (brs, 6H), 3.58 (s, 12H), 2.38 (s, 24H); ^{13}C NMR: $\delta = 146.6$, 130.2, 121.7, 117.1, 59.1, 51.1; MS: *m/z*: 610.4 [$M+H^+$], 632.4 [$M+Na^+$]; elemental analysis calcd (%) for $C_{48}H_{68}N_{12}$: C 70.90, H 8.43, N 20.67; found: C 70.52, H 8.53, N 20.70%.

*1,5,9,13(2)-Tetraamino-1,5,9,13(1,3)-tetrabenzena-3,7,11,13(1,4)-tetrapiperazinacyclophane (**7**)*: Compound **7** was prepared as described above. Macrocycle **4** (0.23 g, 0.24 mmol), tin(II) chloride (2.3 g, 10.2 mmol), and concentrated HCl (2 mL) were used. After reduction, the white solid was filtered and rinsed with acetone and CH_2Cl_2. The solid was mixed with water (100 mL) and neutralized with concentrated aqueous ammonia (20 mL) and extracted into CH_2Cl_2. The crude product was recrystallized from a mixture of CH_2Cl_2 and acetonitrile (1:1; 140 mg, 72%). Decomposition under 300°C; ^{1}H NMR: $\delta = 6.84$ (d, ^3J(H,H) = 7.42 Hz, 8H), 6.57 (t, ^3J(H,H) = 7.42 Hz, 4H), 5.76 (s, 8H), 5.30 (s, 0.5H, CH_2Cl_2), 3.56 (s, 16H), 2.18 (s, 32H), 2.00 ppm (s, 3H, CH_3CN); ^{13}C NMR: $\delta = 146.9$, 130.2, 121.0, 117.0, 61.9, 52.5 ppm; MS: *m/z* = 813.5 [$M+H^+$], 835.5 [$M+Na^+$]; elemental analysis calcd (%) for $C_{48}H_{68}N_{12} \cdot CH_3CN \cdot {}^1/_8 CH_2Cl_2$: C 67.49, H 8.30, N 20.26; found: C 67.77, H 8.67, N 20.12.

Acknowledgements

The financial support from the Academy of Finland (no. 122350 and 113437) and the National Graduate School of Organic Chemistry and Chemical Biology is gratefully acknowledged. We thank Spec. Lab. Technician Reijo Kauppinen for his help in running the NMR spectra. The thank Prof. Pierangelo Metrangolo (Politecnico di Milano, Italy) for the idea of the Pacman analogy.

[1] a) C. Schmidt, T. Straub, D. Falábu, E. Paulus, E. Wegelius, E. Kolehmainen, V. Böhmer, K. Rissanen, W. Vogt. *Eur. J. Org. Chem.* **2000**, 3937–3944; b) A. Shivanyuk, T. P. Spaniol, K. Rissanen, E. Kolehmainen, V. Böhmer, *Angew. Chem.* **2000**, *112*, 3640–3643; c) M. Luostarinen, A. Shivanyuk, K. Rissanen, *Org. Lett.* **2001**, *3*, 4141–4144; d) D. Falábu, A. Shivanyuk, M. Nissinen, K. Rissanen, *Org. Lett.* **2002**, *4*, 3019–3022; e) M. Luostarinen, T. Laitinen, C. A. Schalley, K. Rissanen, *Synthesis* **2004**, 255–262; f) S. Strandman, M. Luostarinen, S. Niemelä, K. Rissanen, H. Tenhu, *J. Polym. Sci. Part A* **2004**, *42*, 4189–4201; g) S. Nummelin, D. Falábu, A. Shivanyuk, K. Rissanen, *Org. Lett.* **2004**, *6*, 2869–2872; h) N. K. Beyeh, D. Fehér, M. Luostarinen, C. A. Schalley, K. Rissanen, *J. Inclusion Phenom. Macrocyclic Chem.* **2006**, *56*, 381–394; i) M. Luostarinen, M. Nissinen, M. Nieger, A. Shivanyuk, K. Rissanen, *Tetrahedron* **2007**, *63*, 1254–1263; j) N. K. Beyeh, J. Aumanen, A. Åhman, M. Luostarinen, H. Mansikkamäki, M. Nissinen, J. Korppi-Tommola, K. Rissanen, *New J. Chem.* **2007**, *31*, 370–376; k) M. Luostarinen, M. Nissinen, H. Lähteenmäki, H. Mansikkamäki, K. Salorinne, C. A. Schalley, K. Rissanen, *J. Inclusion Phenom. Macrocyclic Chem.* **2007**, *58*, 71–80.

[2] a) K. Rissanen, J. Huuskonen, A. Koskinen, *J. Chem. Soc. Chem. Commun.* **1993**, 771–772; b) K. Rissanen, J. Breitenbach, J. Huuskonen, *J. Chem. Soc. Chem. Commun.* **1994**, 1265–1266; c) J. Huuskonen, J. Schulz, K. Rissanen, *Liebigs Ann.* **1995**, 1515–1519; d) J. Huuskonen, J. Schulz, E. Kolehmainen, K. Rissanen, *Chem. Ber.* **1994**, *127*, 2267–2272; e) J. Huuskonen, K. Rissanen, *Liebigs Ann.* **1995**, 1611–1615.

[3] a) A. Ramasubbu, K. P. Wainwright, *J. Chem. Soc. Chem. Commun.* **1982**, 277–278; b) R. D. Hancock, S. M. Dobson, A. Evers, P. W. Wade, M. P. Ngwenya, J. C. A. Boeyens, K. P. Wainwright, *J. Am. Chem. Soc.* **1988**, *110*, 2788–2794; c) K. P. Wainwright, *Inorg. Chem.* **1980**, *19*, 1396–1398.

[4] a) A. Shivanyuk, K Rissanen, E. Kolehmainen, *Chem. Commun.* **2000**, 1107–1108; b) H. Mansikkamäki, M. Nissinen, K. Rissanen, *Chem. Commun.* **2002**, 1902–1903; c) H. Mansikkamäki, M. Nissinen, C. A. Schalley, K. Rissanen, *New J. Chem.* **2003**, 88–97; d) H. Mansikkamäki, M. Nissinen, K. Rissanen, *Angew. Chem.* **2004**, *116*, 1263–1266; e) H. Mansikkamäki, S. Busi, M. Nissinen, A. Åhman, K. Rissanen, *Chem. Eur. J.* **2006**, *12*, 4289–4296.

[5] D. J. Cram, T. Kaneda, R. C. Helgeson, S. B. Brown, C. B. Knobler, E. Maverick, K. N. Trueblood, *J. Am. Chem. Soc.* **1985**, *107*, 3645–3657.

[6] N. Kihara, K. Saigo, Y. Kabata, M. Ohno, M. Hasegawa, *Chem. Lett.* **1989**, 1289–1292.

[7] a) R. D. Hancock, M. P. Ngwenya, A. Evers, P. W. Wade, J. C. A. Boeyens, S. M. Dobson, *Inorg. Chem*, **1990**, *29*, 264–270; b) P. W. Wade, R. D. Hancock, *J. Chem. Soc. Dalton Trans.* **1990**, 1323–1327; c) P. W. Wade, R. D. Hancock, J. C. A. Boeyens, S. M. Dobson, *J. Chem. Soc. Dalton Trans.* **1990**, 483–488.

[8] N. L Allinger, J. G. D. Carpenter, F. M. Karkowski, *J. Am. Chem. Soc.* **1965**, *87*, 1232–1236.

[9] F. R. Fronczek, P. J. Schilling, S. F. Watkins, V. K. Majestic, G. R. Newkome, *Inorg. Chim. Acta* **1996**, *246*, 119–123.

[10] a) R. Gleiter, K. Hövermann, F. Rominger, T. Oeser, *Eur. J. Org. Chem.* **2001**, 725–728; b) E. Krakowiak J. S. Bradshaw, W. Jiang, N. K. Dalley, G. Wu, R. M. Izatt, *J. Org. Chem.* **1991**, *56*, 2675–2680.
[11] a) G. Angelovski, B. Costisella, B. Kolariæ M. Engelhard, P. Eilbracht, *J. Org. Chem.* **2004**, *69*, 5290–5294; M. Engelhard, P. Eilbracht, *J. Org. Chem.* **2004**, *69*, 5290–5294; b) K. Fuji, K. Takasu, H. Miyamoto, K. Tanaka, *Tetrahedron Lett.* **1996**, *37*, 7111–7114.
[12] L. J. Farrugia, *J. Appl. Crystallogr.* **1997**, *30*, 565–566.
[13] A. Bondi, *J. Phys Chem.* **1964**, *68*, 441–451.
[14] G. A. Jeffrey, *An Introduction to Hydrogen Bonding*, OUP, New York, **1997**.
[15] A. L. Spek, *J. Appl. Crystallogr.* **2003**, *36*, 7–13.
[16] Spartan 04, Wavefunction Inc., 18401 Von Karman Ave, Irvine/CA, USA (at DFT, B3LYP, HF 6-31* level of theory)
[17] Pacman, Namco Limited, Japan, released 22.5.1980.
[18] A. Shivanyuk, K. Rissanen, S. K. Korner, D. M Rudkevich, J. Rebek, Jr., *Helvetica Chim. Acta* **2000**, *83*, 1778–1790.
[19] D. Ranganathan, V. Haridas, R. Nagaraj, I. L. Karle, *J. Org. Chem.* **2000**, *65*, 4415–4422.
[20] a) E. Vogel, M. Bröring, J. Fink, D. Rosen, H. Schmickler, J. Lex, K. W. K. Chan, Y-D. Wu, D. A. Plattner, M. Nendel, K. N. Houk, *Angew. Chem.* **1995**, *107*, 2705–2709; *Angew. Chem. Int. Ed. Engl.* **1995**, *34*, 2511–2514; b) M. Bröring, J. Jendny, L. Zander, H. Schmickler, J. Lex, Y-D. Wu, M. Nendel, J. Chen, D. A. Plattner, K. N. H. Houk, E. Vogel, *Angew. Chem.* **1995**, *107*, 2709–2711; *Angew. Chem. Int. Ed. Engl.* **1995**, *34*, 2515–2517; c) J. L. Sessler, S. J. Weghorn, V. Lynch, M. R. Johnson, *Angew. Chem.* **1994**, *106*, 1572–1575; *Angew. Chem. Int. Ed. Engl.* **1994**, *33*, 1509–1512.
[21] M. Mascal, C. J. Moody, A. I. Morrell, A. M. Z. Slawin, D. J. Williams, *J. Am. Chem. Soc.* **1993**, *115*, 813–814.
[22] H. E. Gottlieb, V. Kotlyar, A. Nudelman, *J. Org. Chem.* **1997**, *62*, 7512–7515.
[23] S. Mecozzi, J. Rebek Jr. , *Chem. Eur. J.* **1998**, *4*, 1016–1022.
[24] S. Leon, D. A. Leigh, F. Zerbetto, *Chem. Eur. J.* **2002**, *8*, 4854–4866.
[25] P. Wipf, P. C. Fritch, S. J. Geib, A. M. Sefler, *J. Am. Chem. Soc.* **1998**, *120*, 4105–4112.
[26] K. Boeckmann, F. Vögtle, *Liebigs Ann. Chem.* **1981**, *3*, 467–475.
[27] CCDC-666838, CCDC-666839, CCDC-666840, and CCDC-666841 contain the supplementary crystallographic data for this paper. These data can be obtained free of charge from The Cambridge Crystallographic Data Centre via www.ccdc.cam.ac.uk/data_request/cif.
[28] R. W. Hooft, COLLECT, Nonius BV, Delft (The Netherlands), **1998**.
[29] Z. Otwinowski, W. Minor, *Methods in Enzymology*, **1997**, *276*, Macromolecular Crystallography, Part A, 307–326.
[30] A. Altomare, M. C. Burla, M. Camalli, G. L. Cascarano, C. Giacovazzo, A. Guagliardi, A. G. G. Moliterni, G. Polidori, R. Spagna, *J. Appl. Crystallogr.* **1999**, *32*, 115–119.
[31] L. J. Farrugia, *J. Appl. Crystallogr.* **1999**, *32*, 837–838.
[32] G. M. Sheldrick, SHELXL-97, A program for the Refinement of Crystal Structures, University of Göttingen, Göttingen (Germany), **1997**.
[33] A. Pettit, Y. Iwai, C. F. Barfknecht, D. C. Swenson, *J. Heterocycl. Chem.* **1992**, *29*, 877–881.

Received: November 26, 2007
Published online: February 20, 2008

